Available online at www.sciencedirect.com

ScienceDirect

Procedia CIRP 136 (2025) 325–330

www.elsevier.com/locate/procedia

35th CIRP Design 2025

A method for predicting the dielectric strength of batch MLCCs based on grain structural parameters

Donghui Li[a,b], Yuguang Zhong[a,*], Xue zhou[b], Guofu Zhai[b]

[a] College of mechanical and electrical engineering, Harbin engineering university, Harbin, China.
[b] School of electrical engineering and automation Department, University of Harbin Institute of Technology, Harbin, China.

* Corresponding author. E-mail address: zhongyuguang@hrbeu.edu.cn

Abstract

Multilayer ceramic dielectric capacitor (MLCC) is widely used in circuits, and the dispersion of the ceramic dielectric performance is the main reason for breakdown. In manufacturing, the MLCC quality level is determined by a dielectric breakdown test of some samples taken from a batch. A few studies have built numerical analysis models to calculate the grain size effect on dielectric breakdown, which is more suitable for the specific samples. To face these challenges, this paper establishes a method for predicting the dielectric strength of batch MLCC based on grain structural parameters. This method represents the process influencing the finished dielectric in MLCC by distributing grain size and defects. Then, a graphic model was built to analyze the rule between the dielectric structure and the MLCC dielectric strength. A batch of MLCC was selected as an example, and photographs of dielectric were measured using the watershed algorithm to obtain the distribution of grain sizes and defects, which were used to quickly predict their dielectric strength. Finally, a breakdown test was applied to this batch to verify the validity and accuracy of this method of predicting results.

Keywords: MLCC; Dielectric strength; Graphic Model; Watershed Algorithm;

1. Introduction

Multilayer ceramic dielectric capacitor (MLCC), widely used in electronic devices, significantly impacts the reliability and properties of electronic devices. With electronic devices moving toward miniaturization and high integration, mainly when applied to constellation satellites, unmanned equipment, and new energy vehicles, the failure prediction of MLCC is a great challenge [1]. Due to the large number of MLCC batches produced, some manufacturers try to carry out rapid on-line testing to obtain the breakdown resistance of each MLCC one by one. Limited by the test speed and efficiency requirements, reliance on manufacturing line historical test data remains the predominant approach for MLCC quality characterization. However, this method cannot accurately represent the batch MLCC properties and does not analyze the impact of the manufacturing process on the properties. Thus, the prediction of MLCC properties distribution based on the grain structural parameters is helpful for the quality analysis and design process.

In many studies on multilayer ceramic capacitors, the enhancement of material properties has been the central theme. Zhang et al. [2] doped Co_2O_3 in $BaTiO_3$ to improve the material properties and used X-ray photoelectron spectroscopy (XPS) to measure the optimized material and demonstrate that introducing Co could improve the reduction resistance of BT-based ceramics. Muhammad et al. [3] improved the dielectric properties and thermal stability by adding $NaNbO_3$ to $BaTiO_3$. It founds that this method significantly improved the material's dielectric stability and energy storage density. This type of study can effectively enhance the breakdown resistance of MLCC by improving the materials. However, these studies

10.1016/j.procir.2025.08.057

have some limitations, and the impact of material improvement on MLCC fabrication costs must be addressed.

Regarding failure analysis of MLCC, the traditional accelerated degradation test is still the primary research method to evaluate their performance. Yang et al. [4] explored the application of MLCC in automotive engine control units through failure analysis and reliability estimation. After identifying the main failure modes of relocated MLCC, they proposed a Prokopowicz-Vaskas life model based on the Weibull distribution based on accelerated life test data. Saito et al. [5] investigated the effect of water vapor infiltration on the leakage current of MLCC under high accelerated temperatures and humidity environments. The study used heavy water as a tracer and detected water vapor permeation in MLCC by secondary ion mass spectrometry. The results show that water vapor permeation does increase the leakage current of MLCC, a finding that provides an experimental basis for the electrical breakdown failure mechanism of MLCC. On the other hand, Hong et al. [6] focus on the metal-ion migration process of MLCC applied to automobiles. He analyzes the failure time of MLCC under different environmental conditions through temperature-humidity-bias (THB) tests. Based on the degradation test data designed by Taguchi's method, Bhargava et al. [7] trained an Artificial Neural Network (ANN) to analyze the reliability of MLCC. The regression analysis and ANN achieved 97.05% and 94.07% accuracy, respectively, indicating the effectiveness of neural networks in solving the MLCC failure problem. Wang et al. [8] investigated the insulation reliability of MLCC by highly accelerated life testing (HALT). Based on the test results of HALT, this study used Kaplan-Meier survival analysis, Weibull distribution fitting, and genetic algorithm to calculate the mean time to failure (MTTF) of MLCC under HALT conditions and compared the fitting effects of different methods. The study proposes a method to evaluate the reliability characteristics of the samples using a bath curve. The evaluation results determine the optimal sintering temperature scheme for the capacitors. Zhu et al. [9] investigated the degradation mechanism of ultra-thin-layer MLCC using an accelerated aging test system. In the accelerated aging test, the ceramic dielectric was degraded by the applied stringent electric field and temperature drop, and the oxygen vacancies gradually migrated in the grains, penetrated through the crystals, and finally accumulated near the cathode. As a result, a semiconductor layer with poor insulating properties is formed near the cathode, and the height of the potential barrier at the interface decreases. Therefore, suppressing the migration and enrichment of oxygen vacancies is a top priority to ensure the reliability of MLCC. Although such studies can establish life prediction models based on accelerated life test data, most focus on specific application scenarios and lack linkage to MLCC structures and parameters.

Compared to the degradation of MLCC performance caused by long-term operation, voltage breakdown failure will directly cause damage to MLCC, resulting in short-circuit or open-circuit failures. Yoon et al. [10] investigated the AC and DC breakdown characteristics of MLCC at high voltages. They found that the dielectric thickness and the shape of the internal electrodes influence the breakdown voltage. Xia et al. [11] investigated the failure modes of MLCC under pulsed voltage conditions, and obtained the breakdown paths based on the weak point breakdown theory and electric tree model.

In numerical analysis, Allen Templeton et al. [12] studied the breakdown of MLCC in high-switching frequency circuits. They used ANSYS to build a finite element model to calculate the current density distribution of MLCC based on measured voltage loads. They found that high dV/dt pulses induced internal stresses in the MLCC, but the performance of the capacitors was not degraded after testing. Lei et al. [13] performed coupled electrical-thermal-force multi-physics field numerical simulations of a nonlinear, high-voltage ceramic capacitor using COMSOL Multiphysics to approximate the capacitor's real-world operating conditions. They investigated the electric, temperature, and stress field distributions of the capacitors under standard operating shock voltage waveforms. They found that the cracking of copper terminals and silver electrodes due to temperature effects may be the leading cause of failure. Mohammad et al. [14] simulated the breakdown process of polycrystalline ferroelectrics using the phase field method. This study analyzed the effect of parameters such as grain orientation, dielectric constant of grains and grain boundaries, grain boundary thickness, and grain size on the threshold breakdown electric field. This study found that the decrease in dielectric constant will enhance the threshold dielectric strength of the material.

In manufacturing, the MLCC quality level is determined by breakdown tests on samples taken from a batch. While sampling tests can evaluate the quality of MLCCs, they cannot help the design process. To address this challenge, this paper presents a method to predict the dielectric strength of MLCCs based on grain structural parameters. This method uses multi-scale retinex with color restoration (MSRCR) and watershed algorithm to improve the quality of the photos and identify the grains and pores. Then, the distribution of grain size and pores are statistically calculated, and a graph-equivalent model reflecting the microstructure in the dielectric is established. Based on the measured breakdown voltage and the breakdown path length, the dielectric strength of MLCC was calculated. Finally, MLCC samples were selected for breakdown tests to verify the effectiveness of this method.

2. Methodology

2.1. Method flow

It has been pointed out that the dielectric thickness, grain size, and defects are the main factors affecting the breakdown of MLCC [15-18]. Due to the inherent variability associated with the manufacturing process, accurately calculating the microstructure of MLCC dielectrics based solely on process parameters presents significant challenges. Currently, manufacturers mainly obtain the dielectric structure characteristics by DPA (Destructive physical analysis)and statistically analyzing scanning electron microscope (SEM) photos [19]. Limited by measurement ability and testing efficiency, manufacturers focus only on significant defects in

the dielectric, and blurrier SEM photos have met this demand. Stacked grains make the grain boundaries challenging to identify, increasing the difficulty of micro-structure identification.

This paper uses the MSRCR algorithm to improve the quality of the original photos and make the grains and pores more significant. The watershed algorithm, a classical image segmentation technique in computer vision [20], delineated grain boundaries in SEM micrographs. This method treats image intensity gradients as topographic surfaces, simulating fluid flooding from regional minima to partition adjacent structures [21]. The watershed algorithm segments the boundaries between grains, while morphological processing is used to repair holes in objects and remove noise. The object is recognized by specifying the connectivity region, and the grain and pore distributions are statistically obtained and fitted. A Voronoi diagram of grain boundary paths is created based on the probability of pore occurrence and the pore area. Paths in the Voronoi Diagram where pores may exist are marked to simulate the impact of pores on the dielectric. An equivalent graphical model describing the paths is created by using the intersections of the grain boundaries as nodes, each boundary length as the weight, and lowering the weight at the pores. After completing the above, Dijkstra's algorithm finds the path with the smallest weight sum in the graphical model as the breakdown path. Finally, the dielectric strength of the MLCC is calculated based on the measured voltage of the samples. The whole process is shown in Fig. 1.

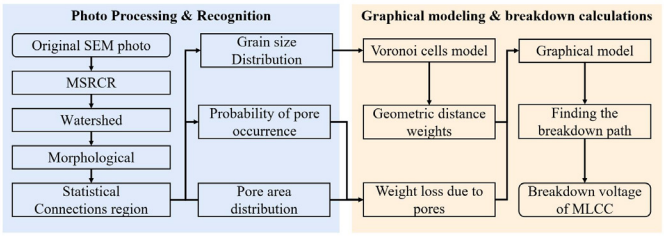

Fig. 1. Methodological process

2.2. MSRCR and the Watershed Algorithm

In SEM photos, all clear grains can be approximated as being in the same plane, thus allowing statistical characterization of the dielectric micro-structure. MSRCR is a general-purpose image enhancement algorithm that can provide both local brightness and contrast enhancement and has been successfully applied in different fields. For blurring small particles, such as the dielectric microstructure, MSRCR can effectively improve the clarity of the photos. The output result R_i on pixel (x_1,x_2) after MSRCR is[22]:

$$R_i(x_1,x_2)=\gamma_i(x_1,x_2)\sum_{k=1}^{K}W_k\left(\log\left(I_i(x_1,x_2)\right)\right) - \log\left[I_i(x_1,x_2)*F_k(x_1,x_2)\right] \quad (1)$$

where, subscript i denotes the i-th spectral band, (x_1, x_2) is the pixel position on the image, γ is the color restoration factor, K is the number of surround functions or scales, I is the input image, F_k denotes the k-th surround function, $W_k = 1/3$ is the weights associated with F_k, and * denotes convolutional operator.

After ensuring the clarity of the photos, there is a need to focus on the blurring of grain boundaries caused by stacking in the photos. First, the endpoint locations must determined by the specified linkage structure. Then, the existing edge pixel positions are fitted to obtain the slope of the existing boundary at the endpoint. The boundary is iteratively expanded based on the slope until another endpoint is encountered to complete the edge detection and populate the object. When splitting the connected grains in the image, the gray value, size, and shape that matches the grain boundary structure can be selected as watershed markers [22]. Finally, depending on the results of the image, morphological methods can be used to erode or dilate the subjects to further improve the quality of the image. An MLCC is used as an example to illustrate this process. The dielectric is strontium titanate, and its dielectric layer is designed to be 31.2 μm. Based on the results in Fig. 2, it can be found that the identified grains match well with the original photo, which indicates the effectiveness of the method for the micro-structure structural identification.

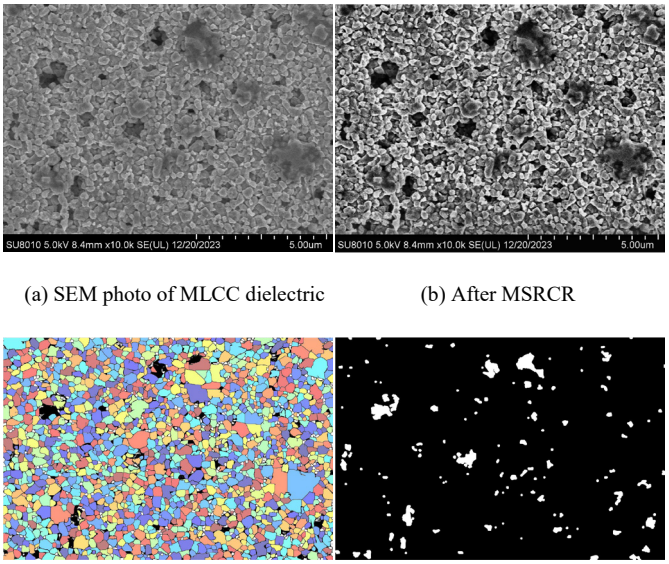

(a) SEM photo of MLCC dielectric (b) After MSRCR

(c) Identified grains on original photos (d) Pores obtained from morphology

Fig .2. Identification process of MLCC dielectric structure

2.3. Calculating dielectric strength

Influenced by manufacturing process-induced defects and higher electric fields, the dielectric breakdown along the grain boundaries when the electric field is higher than the dielectric strength. [16] In contrast to Joule breakdown due to slow degradation, dielectric breakdown is only related to the dielectric strength. When an MLCC breaks at voltage V, the dielectric strength is calculated as shown below[23-24]:

$$E_b = V/(d_0 - d_p) \quad (2)$$

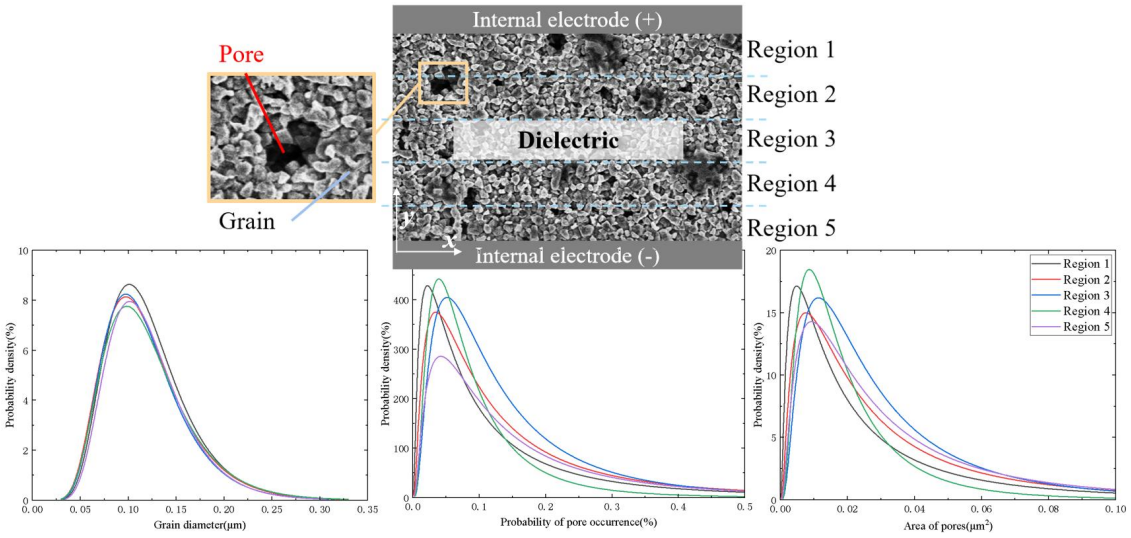

Fig. 3. Statistical results on microstructure of dielectric

where, d_0 is the shortest distance between electrodes along the grain boundary in the dielectric, which is determined by the probability of the grain size r_g, d_p is the shortest distance caused by defects, which is together defined by the probability of the pore occurrence o_p, and the probability of the pore size r_p, E_b is the dielectric strength.

3. Results

3.1. Results for batch samples

The CT41-1206-50V-475 was chosen as a sample to illustrate the prediction ability for batch products, whose designed dielectric thickness was 4.25 μm. The samples of cut MLCC sections were photographed at 10k magnification using a SEM (SU8010, HITACHI). To reflect the defect-prone phenomenon at the interface between the dielectric and the inner electrode, the dielectric is divided equally into five regions along the thickness, and the microstructure is counted separately in the figure. Based on the flow in Fig. 1, the program was run in GNU Octave 9.2.0, and statistics on the distribution of grain structural parameters in the images.

The grain size probability density of the medium, r_g, the pore size probability density, r_p, and the probability density of pore occurrence (the proportion of pore area to the region), o_p, are shown in Fig. 3. The parameters follow the lognormal distribution, and they were used to create Voronoi diagram and transformed into the equivalent graphical model. The equivalent graphical model based on grain size, pore size, and pore occurrence probability is shown in Fig. 4. The nodes located on the inner electrode (-) are the entrances. The nodes on the inner electrode (+) are the exits, and the shortest path is found based on the grain boundary weights, as shown in Fig. 5. Although there is a shorter path in the dielectric, the breakdown path is impacted by the reduced weights caused by the pores.

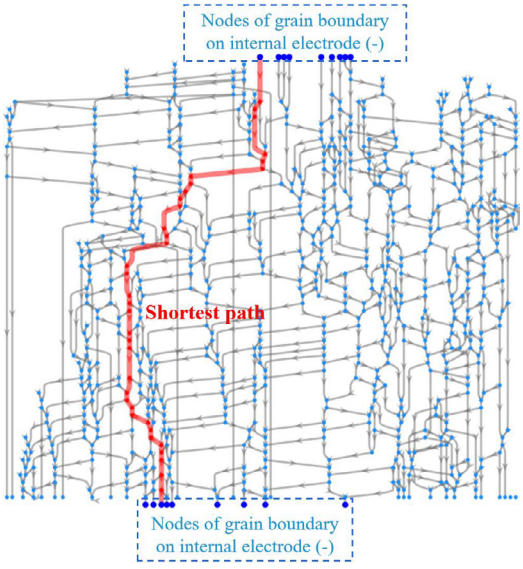

Fig. 4. The shortest path on the graphical model

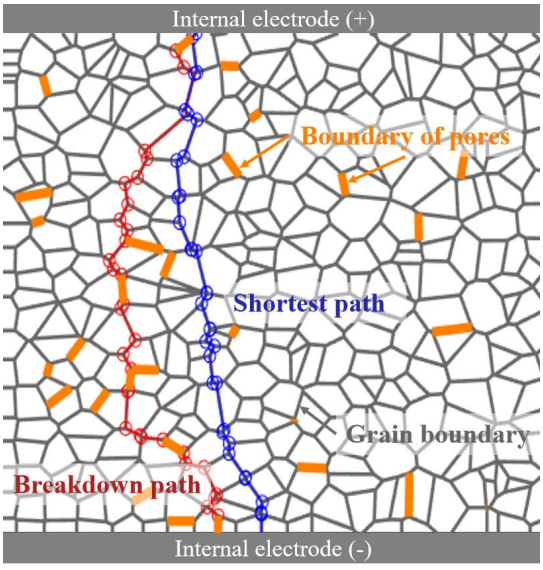

Fig. 5 The shortest path on the dielectric virtual sample

Based on the grain size probability density r_g, the pore size probability density r_p, and the pore occurrence probability o_p 100 virtual samples are constructed to statistically the breakdown path lengths when only the grain size and when the pore size is taken into consideration. Based on the experimentally measured average dielectric strength and the breakdown path lengths from the virtual samples, the predicted results of the dielectric strength distribution are shown in Fig. 6. In the prediction using only grain size, the dielectric strength ranged from 107.81 V/um to 118.98 V/um. The dielectric strength ranged from 107.62 V/um to 139.26 V/um when using grain size and pore properties. A sample of 100 MLCCs was selected randomly from a batch, and a breakdown test was carried out on them to verify the validity of this method. In the test, the breakdown voltage of the samples ranged from 454.75 V to 590.75 V, and the dielectric strength could be approximated to range from 107 V/um to 139 V/um. Compared to using only grain size, the prediction method using both grain size and pore properties is significantly closer to the test results, which shows the effectiveness of the present method.

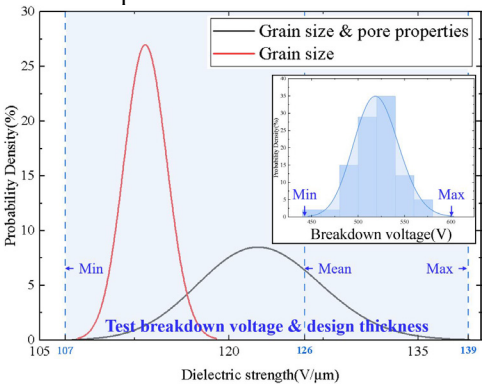

Fig. 6 Calculated results of dielectric strength

3.2. Results for different methods

To verify that this method also applies to MLCCs with different grain structural parameters, an additional type, CT41-0805-50V-222, was selected as the sample. This MLCC is made of strontium titanate, and the designed dielectric thickness is 31.2 μm. After the same analytical steps, the dielectric strength results are shown in Fig. 7.

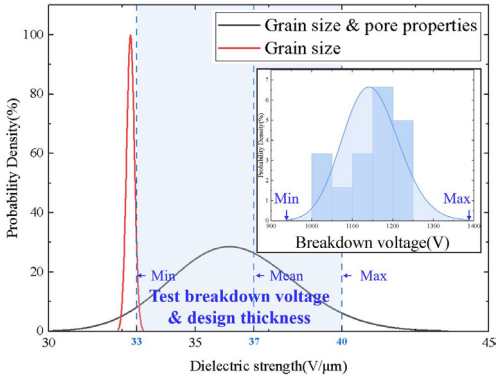

Fig. 7. Calculated results of CT41-0805-50V-222

Unlike the sample selected in the previous section, this sample requires a much higher energy density due to the smaller package, resulting in increased dielectric thickness and layers. This design also increases the uncertainty of the microstructure in the dielectric, and it will be easier to encounter more pores in the breakdown path, as shown by the wider breakdown voltage range (940V~1380V).

4. Discussion

This paper presents a methodology that solves the challenge of predicting the MLCC dielectric strength. Two examples of its application on different products validate the methodology. Due to the short time of this work, some limitations and directions for follow-up work still need to be discussed:

- In this paper, SEM photos provided by the manufacturer were processed by MSRCR to improve clarity, and the watershed algorithm segmented the stacked grains. In this work step, statistical errors may be induced by the over-concentration regions measured by the SEM. Limited by the stacking manufacturing process of MLCC, more pores may exist in the dielectric near the internal electrode. In future work, the SEM measurement regions will be increased, and try to add the regional and spatial coordinates to the probability density function of grain size and porosity.
- This paper assumes that the electric field is equal on the breakdown path in calculating the dielectric strength. Although the test results indicate that the predicted dispersion of dielectric strength is more accurate, it can be applied in engineering. However, this simplified calculation ignores the electric field distribution, which limits this method in the study of dielectric breakdown path spreading. The next step will be to combine this method with the phase field method by considering the energy conversion in dielectric breakdown.
- Based on the test results of the two samples, the dielectric breakdown strength is lower for MLCCs with higher energy density. This is because the increase in energy density increases the number of grains in the dielectric, and the accompanying increase in pores reduces the grain boundary ratio in the breakdown path. On the other hand, if only the grain boundary length is considered and the effect of pores is ignored, the MLCCs with higher energy density have a lower dispersion of grain boundary lengths and are closer to the design thickness. This also indicates that when the energy density of MLCC is lower, its dielectric strength is affected mainly by the grain boundary length on the breakdown path. And when the energy density of MLCC is higher, the pores are the main reason for the dielectric strength.

5. Conclusions

This paper focuses on the challenges of addressing and evaluating the effects of grain structural parameters on the dielectric breakdown of MLCCs. It presents a methodology

for predicting the dielectric strength based on the microstructure in the dielectric layer. In addition, the impact of grain structural parameters on MLCC dielectric breakdown is also initially explored to help in design and failure analysis.

- Compared to using the design thickness to calculate the dielectric strength, this method can predict the parameter distribution of a batch based on the grain structural parameters without depending on a large number of samples. In contrast to the dielectric strength calculation method that only considers the grain size, the range of dielectric breakdown strength predicted by the proposed method can cover the distribution of the test results. In addition, the more conservative dielectric strength prediction results make the present method more suitable for engineering applications.
- The dielectric strength of an MLCC is related to its energy density, specifically through the number of pores in the dielectric causing an effect. When the energy density of MLCC is lower, its dielectric strength is affected mainly by the grain boundary length on the breakdown path. And when the energy density of MLCC is higher, the pores are the main reason for the dielectric strength.

Acknowledgements

This work was supported by the National Natural Science Foundation of China 52177133 and 52375490.

References

[1] Laadjal K, Cardoso AM. Multilayer ceramic capacitors: an overview of failure mechanisms, Perspectives. and Challenges. Electronics 2023; 12(6):1297.

[2] Zhang J, Hao H, et al. Dielectric and anti-reduction properties of BaTiO3-based ceramics for MLCC application. Ceramics International 2023; 49(15):24941-24947.

[3] Muhammad R, Ali A, et al. Enhanced thermal stability in dielectric properties of NaNbO3-modified BaTiO3-BiMg1/2Ti1/2O3 ceramics for X9R-MLCC applications. Crystals 2022; 12(2):141.

[4] Yang S, Kim JW, et al. Reliability estimation and failure analysis of multilayer ceramic chip capacitors. International Journal of Modern Physics B 2003; 17(8-9):1318-1323.

[5] Saito Y, Oguni T, et al. Infiltration of water vapor into multi-layer ceramic capacitors under highly accelerated temperature and humidity stress tests. Applied Physics Express 2021; 14(5):051005.

[6] Hong WS, Kim MS, et al. Electrochemical metallic ion migration property of multi-layer ceramic capacitor for car electronics. Journal of Welding and Joining 2023; 41(6):519-527.

[7] Bhargava C, Sharma P. Statistical and intelligent reliability analysis of multi-layer ceramic capacitor for ground mobile applications using Taguchi's approach. International Journal of Quality and Reliability Management 2022; 39(10):2273-2285.

[8] Wang Z, Yan S, et al. Using highly accelerated life test to study insulation reliability of multi-layer ceramic capacitors sintered at different temperatures. Journal of Applied Physics 2024; 135(2):029901.

[9] Zhu C, Cai Z, et al. Reliability mechanisms of the ultrathin-layered BaTiO3-Based BME MLCC. Acta Physico Chimica Sinica 2024; 40(1):202304015.

[10] Yoon JR, Kim MK, Lee SW. The AC, DC dielectric breakdown characteristics according to dielectric thickness and inner electrode pattern of high voltage multilayer ceramic capacitor. Journal of The Korean Institute of Electrical and Electronic Material Engineers 2008; 21(12):1118-1123.

[11] Xia J, Cao F, Chen X, et al. Investigation on discharge behavior of antiferroelectric multilayer ceramic capacitors. IEEE Transactions on Dielectrics and Electrical Insulation 2023; 30(2):643-648.

[12] Templeton A, Reed N, et al. Class I multi-Layer ceramic capacitors (MLCCs) performance as wide band gap (WBG) Snubbers in Hard Switching Applications. 2023 Fourth International Symposium on 3D Power Electronics Integration and Manufacturing (3D-PEIM) 2023;

[13] Yu-Xing L, Yan Xue-yang, et al. Multi-physical field simulation of nonlinear high-voltage ceramic capacitor based on COMSOL. 2022 4th International Conference on Smart Power and Internet Energy Systems (SPIES) 2022.

[14] M Khondabi, H Ahmadvand, M Javanbakht. Revisiting the dielectric breakdown in a polycrystalline ferroelectric: a phase-field simulation study. Adbanced theory and simulations 2023; 6(1):2200314.

[15] FZ Yao, QB Yuan, Q Wang. Multiscale structural engineering of dielectric ceramics for energy storage applications: from bulk to thin films. Nanoscale 2020; 12(33):17165-17184.

[16] C Zhu, Z Cai, L Guo, et al. Grain size engineered high-performance nanograined BaTiO3-based ceramics: experimental and numerical prediction. Journal of the American ceramic society 2021. 104(1):273-283.

[17] B Liu, X Wang, R Zhang, et al. Grain size effect and microstructure influence on the energy storage properties of fine-grained BaTiO3-based ceramics. Journal of the American ceramic society 2017; 100(8):3599-3607.

[18] SC Lu, YH Chen, et al. Effect of microstructure on dielectric and fatigue strengths of BaTiO3. Journal of the European ceramic society 2010; 30(12):2569-2576.

[19] LW Wu, ZM Cai, CQ Zhu. Significantly enhanced dielectric breakdown strength of ferroelectric energy-storage ceramics via grain size uniformity control: phase-field simulation and experimental realization. Applied physics lettrs 2020; 117(21):212902

[20] Beucher S. Watershed, hierarchical segmentation and waterfall algorithm. Mathematical Morphology and Its Applications to Image Processing 1994; 2(9):69-76.

[21] JBTM Roerdink, A. Meijster. The watershed transform: definitions, algorithms and parallellization strategies. Fundamenta Informaticae 2000; 41(2):187-228.

[22] B Jiang, GA Woodell, DJ Jpbson. Novel multi-scale retinex with color restoration on graphics processing unit. Journal of real-time image processing 2015; 10(2):239-253

[23] HS Chuang, CH Lin. Automated grain sizing using mark-based watershed algorithm. IEEE International Symposium on Geoscience and Remote Sensing IGARSS 201; 2332-2335.

[24] ZM Cai, XH Wang, LT Li. Phase-field modeling of electromechanical breakdown in multilayer ceramic capacitors. Advanced theory and simulations2019; 2(4):1800179.